

Study on controlled drug permeation of magnetic-sensitive ferrogels: Effect of Fe₃O₄ and PVA

Ting-Yu Liu, Shang-Hsiu Hu, Kun-Ho Liu, Dean-Mo Liu, San-Yuan Chen*

Department of Materials Sciences and Engineering, National Chiao Tung University, Hsinchu, 300, Taiwan, ROC

Received 29 June 2007; accepted 5 December 2007

Available online 15 December 2007

Abstract

A PVA-based magnetic-sensitive hydrogel (ferrogel) was fabricated by physical cross-linking through a freezing–thawing method. The influence of the constituting components, i.e., Fe₃O₄ and PVA, on the magnetic-sensitive behavior of the ferrogels was systematically investigated in terms of permeability coefficient (P), partition coefficient (H), space restriction and magnetization. The results show that, the P value in these ferrogels decreases and displays a magnetic sensitivity when it is subjected to magnetic field (MF), which is correlated with the change of H value. In addition, it was found that although the factor of space restriction or magnetization exerts opposite effect on resulting magnetic-sensitive behavior, the superior magnetic-sensitive behavior was observed for the ferrogels with an optimal composition of 17–34% Fe₃O₄ and 10–12.5% PVA, and can be well correlated with theoretical calculation from the critical parameters of available free volume per nanoparticle (V_{free}) and magnetization. A map of magnetic-sensitive behavior was constructed, where a region with relatively stable and highly stimuli-responsive behavior in terms of the concentration of Fe₃O₄ was observed, however, below or above the “saturation” region (17–34% Fe₃O₄), a reduction in the magnetic-sensitive behavior was detected. The resulting ferrogels can be engineered with a precise control of the opening and closure of pore configuration, which allows a burst release or no-release action of therapeutically active agent to be controlled externally and magnetically. This suggests that this type of ferrogel can be considered as a class of novel magnetically-tunable drug delivery system.

© 2007 Elsevier B.V. All rights reserved.

Keywords: PVA; Fe₃O₄ nanoparticles; Magnetic hydrogel (ferrogel); Controlled permeation

1. Introduction

Certain polymer gels represent one class of actuators that have the unique ability to change elastic and swelling properties in a reversible manner. Volumetric phase transition in response to an infinitesimal change of external stimuli, such as pH, temperature, electric and magnetic field (MF) in various hydrogels has been observed [1–10]. In order to accelerate the response of an adaptive hydrogel to stimuli, a magnetic-sensitive hydrogel (ferrogel) has been developed. A ferrogel is a physical (or chemical) cross-linked polymer network containing magnetic particles. Magnetic-field sensitive gels are unique materials

in that they are mechanically soft and highly elastic and at the same time they exhibit a strong magnetic response.

The principle of shape deformation and motility of ferrogels in response to drug release is based on their unique magnetic-elastic behavior. Gel motions are driven and controlled by MF and the final shape is determined by a balance of magnetic and elastic interaction [11]. Recently, some magnetic-stimuli in response to drug delivery have been applied in clinical therapy. For example, the polyelectrolyte microcapsules embedded with Co/Au nanoparticles could increase its permeability (P) to macromolecules like FITC-labeled dextran by alternating current (AC) magnetic switch [12]. Saslawski et al. reported the gelatin microsphere that was cross-linked by polyethylenimine for the pulsed delivery of insulin by oscillating MF [13]. However, little investigation has been reported on controlled permeation of drugs under the direct current (DC) MF through the controlled deformation of ferrogels upon a simple “on” and

* Corresponding author. Tel.: +886 3 5731818; fax: +886 3 5725490.

E-mail address: sanyuanchen@mail.nctu.edu.tw (S.-Y. Chen).

“off” switch mode. In our previous work, the bursting and magnetic-sensitive behaviors of PVA-based ferrogels were investigated with various particle sizes of Fe_3O_4 and switching duration time of magnetic fields [14]. From our previous experimental observation, it was found that permeation rate of vitamin B_{12} , as a model molecule, decreased with the increased intensity of direct current (DC) magnetic field. This induces the Fe_3O_4 particles within the ferrogel to aggregate together instantly, leading to a rapid decrease in the porosity of the ferrogel, where the ferrogel was characterized as a “close” configuration [14,15]. In other words, while the imposed field induces magnetic dipoles, mutual particle interactions occur if the particles are so closely packed that the local field can influence their neighbors. The particles attract with each other when aligned in an end-to-end configuration and thus a “pearl-chain structure” was developed [16]. Therefore, the drugs are restrictedly confined in the network of the ferrogels, causing a rapid and significant reduction in the diffusion of the drug from the ferrogel, due to the attractive forces that reduced the pore size of the ferrogel. While turning off the field, the pores in the ferrogel re-open instantly, the drug release turned back to normal diffusion profile.

The above-mentioned phenomenon indicates that the optimal magnetic-sensitive behavior of the ferrogel was not only dependent on the particle size of Fe_3O_4 but also on the constituting components, i.e., Fe_3O_4 and PVA. Therefore, the influence of the respective constituting components of the ferrogels on magnetic-sensitive behavior and partition coefficient (H) will be systematically investigated in this work. These magnetic-sensitive behaviors will be further correlated with theoretical calculation of both space restriction and magnetization. According to the proposed model, an optimal scenario from both experimental findings and calculations would be deduced to fabricate a ferrogel with controlled smart configuration.

2. Materials and methods

2.1. Ferrogel preparation

A freezing–thawing technique was used to prepare the ferrogel [17]. In our experience, the physical-cross-linked ferrogel by a freezing–thawing technique was used in the present study because it presents more elastic and soft properties than that fabricated by chemical-cross-linking. First, various weight/volume (w/v)% of polyvinyl alcohol (PVA, Fluka, M.W.: 72,000, degree of hydrolysis: 97.5–99.5 mol%) was dissolved in 10 ml dimethylsulfoxide (DMSO) at 80 °C under stirring for 6h, and then mixed with various (w/v)% of magnetic particles at 60 °C under ultrasonication for 6h to ensure that the magnetic particles (diameter ca. 150–500 nm, Aldrich) can be well-dispersed, as shown in Table 1. The resulting solution was then poured into plastic dish and kept frozen at –20 °C for 16 h. Subsequently, the gels were thawed at 25 °C for 5 h. This cyclic process including freezing and thawing was repeated for 5 times. Finally, prior to the release test, the ferrogels were washed five

Table 1

Average permeability coefficient (P) of the ferrogels at a given magnetic field

Ferrogels	PVA (w/v)% ^a	Fe_3O_4 (w/v)% ^a	P_{ON} ^b	P_{OFF} ^c	$\Delta P_{\text{OFF-ON}}$ ^d
Pure PVA10	10	–	54±3	54±5	0
PVA10-MP3.75	10	3.75	123±6	172±9	49
PVA10-MP8.5	10	8.5	86±9	170±5	84
PVA10-MP17	10	17	54±9	161±12	107
PVA10-MP25.5	10	25.5	43±11	154±5	111
PVA10-MP34	10	34	31±5	141±7	110
PVA10-MP51	10	51	40±8	131±9	91
PVA10-MP68	10	68	45±6	117±5	72

^a (w/v)% means the weight/volume percentage (weight of PVA or Fe_3O_4 particles/volume of DMSO (v)), ex. 1 g of PVA and 10 ml of DMSO is 10 (w/v)% of the column of PVA (w/v)%.

^b Average permeability coefficient (10^{-6} cm²/min) at magnetic fields switching “on” (MF ON) ($n=3$).

^c Average permeability coefficient (10^{-6} cm²/min) at magnetic fields switching “off” (MF OFF) ($n=3$).

^d Magnetic-sensitive behaviors: average permeability coefficient (10^{-6} cm²/min) at MF OFF – average permeability coefficient (10^{-6} cm²/min) at MF ON. ($n=3$).

times and then immersed in the water for 24 h to completely remove DMSO.

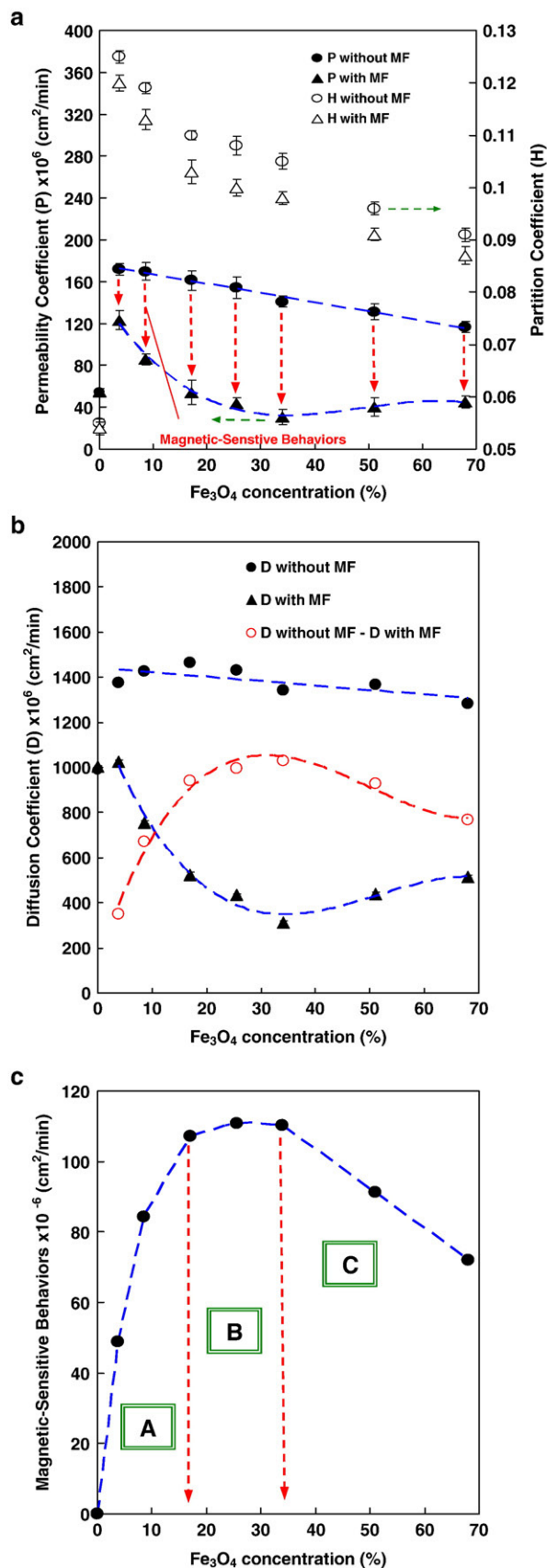
2.2. Diffusion characterizations

The diffusion coefficients of the solutes were measured under switching MF (magnetic strength of about 400 Oe measured by Gauss meter) in a diffusion diaphragm cell (side-by-side cell) [14]. The solution in the donor side is 80 ml of isotonic phosphate buffer (PBS) (pH 7.4) containing 200 ppm of the model drug (vitamin B_{12}). The receptor compartment, separated by the ferrogel, was filled with 80 ml of PBS solution. The concentration of each compound in the receptor compartment was determined at $\lambda=361$ nm using a UV spectrophotometer. The permeation coefficient (P , cm²/min) was calculated according to the following equation for the diaphragm cell:

$$\ln\left(\frac{C_{\text{d0}}}{C_{\text{d}} - C_{\text{r}}}\right) = \frac{2[DH]At}{\delta V}, (P = DH) \quad (1)$$

where C_{d0} is the initial concentration of the permeant in the donor compartment; C_{d} and C_{r} are indicative of the concentrations in the donor side and receptor side, respectively; D is the diffusion coefficient (cm²/min) [18–21]; H is the partition coefficient; A is the effective area of the ferrogel; δ is the thickness of the ferrogel; V are respectively the volumes of solution in the donor and receptor compartment (both are 80 ml). By plotting $\ln[C_{\text{d0}}/(C_{\text{d}} - C_{\text{r}})]$ versus time (t), the permeability coefficient (P) can be calculated from the slope of the line by Eq. (1). Each data point was obtained by averaging of at least three measurements.

Moreover, the dry weight (W_{dry}) of drug-free ferrogel was immersed in the release medium until equilibrium state and then the wet weight (W_{wet}) was recorded. Subsequently, the ferrogel was immersed in 10 ml of vitamin B_{12} -containing medium.



Partition coefficient (H) was determined from the initial (C_0) and equilibrium (C_e) concentrations of vitamin B12-containing mediums by Eq. (2) [20,21].

$$H = \frac{W_{\text{dry}}(C_0 - C_e)}{W_{\text{wet}}C_e} \quad (2)$$

2.3. Porosity determination [19]

The porosity of the ferrogels was determined by measuring the true density and the bulk density. To measure the true density, a freeze-dried ferrogels were placed in a vacuum oven and the weight of the sample was measured (M). Afterwards, the ferrogels were put into the cell chamber cup of a pycnometer (Micromeritics, 1305) to measure the true volume (V_t). The true density (ρ_t) was then calculated according to Eq. (3). To measure the bulk density, ferrogels were vacuum dried and then the area was measured. The thickness of the ferrogels was measured ten times with a digital gauge meter (Mitutoyo IDF-112) to obtain the bulk volume (V_b). The bulk density (ρ_b) was then calculated according to Eq. (4). The porosity (ε) of the ferrogels was calculated according to Eq. (5).

$$\rho_t = M/V_t \quad (3)$$

$$\rho_b = M/V_b \quad (4)$$

$$\varepsilon = V_{\text{bulk}}/V_{\text{true}} - 1 \quad (5)$$

3. Results and discussion

3.1. Role of iron oxide content

According to our pervious study [14], it was found that the larger magnetic particles exhibited better magnetic-sensitive behaviors. Therefore, magnetic particles with size between 150 and 500 nm were employed in the present investigation. Table 1 gives a series of resulting average P values of the ferrogels with a number of Fe₃O₄ concentrations at a given amount of PVA concentration. The influence of Fe₃O₄ concentration is then constructed into Fig. 1(a) with respect to a corresponding change of the P value upon on–off operation of the MF.

As shown in Fig. 1(a), as the Fe₃O₄ nanoparticles were added into the PVA, the P value was much increased compared to that of pure PVA. It was found that the P value in the ferrogel membrane with only 3.75 w/v% Fe₃O₄ is more than 3 times permeable to vitamin B₁₂ than that of pure PVA in the absence of MF. However, with the increase of Fe₃O₄ addition, the P value decreased linearly and slowly with Fe₃O₄ concentration in the absence of magnetic fields (P_{OFF}). In contrast, the drug permeation in the presence of magnetic fields (P_{ON}) decreased

Fig. 1. (a) Both permeability coefficient (P) and partition coefficient (H) of ferrogels in “on” or “off” mode of a given magnetic field; (b) Diffusion coefficient (D) of ferrogels in “on” or “off” mode of a given magnetic field; (c) Magnetic-sensitive behaviors of ferrogels with different Fe₃O₄ concentration; Region A: region of increasing “sensitivity”; Region B: saturation region; Region C: region of decreasing “sensitivity”.

rapidly with Fe₃O₄ up to 34%, then, increased slightly with further increase to 68%. A plethora of Fe₃O₄ (51% and 68%) added in the PVA hydrogel caused a phase separation of PVA to form broken pores; P_{ON} thus increased slightly in the later half. It was believed that there exists a relationship between the P and H value of the drug inside the membrane (see Eq. (1), where $P=DH$). As illustrated in Fig. 1(a), when a smaller amount of 3.75 w/v% Fe₃O₄ particles was added into PVA (ex. PVA10-MP3.75), it caused a considerable increase (2.3 times) in the H value (0.125) compared to that (0.055) in the pure PVA hydrogel. It is then suggested that the addition of iron oxide nanoparticles in the membrane may induce higher porosity to promote the ability of drug absorption of the ferrogel. However, it was observed that the H value decreased with increasing Fe₃O₄ contents. Especially in the presence of MF, the decrease in the H value becomes more remarkable compared to that in the absence of MF. The decreased H value in the presence of MF is probably related to the shrunk volume of ferrogels induced by Fe₃O₄ nanoparticles aggregation to further decrease the pore size and porosity. From above-mentioned results, it can be inferred that the magnetic-sensitive behaviors, i.e., the difference in the P value between MF “on” and “off” modes were primarily affected by the change of H and D value, especially D value (for the concentration of 34%, $\Delta P_{OFF-ON}/P_{OFF} = 110/141 = 0.78$, whereas $\Delta H_{OFF-ON}/H_{OFF} = 0.01/0.11 = 0.09$). The influence of Fe₃O₄ concentration value on the corresponding change of D value is then constructed into Fig. 1(b) upon on–off operation of the MF (D_{ON} and D_{OFF}). It could be found that the D curves show similar trend to the P ones. The D value decreased slightly with Fe₃O₄ concentration in the D_{ON} , but decreased rapidly with Fe₃O₄ up to 34%, then, increased slightly with further increase to 68% in the D_{OFF} . A plateau of magnetic-sensitive behavior ($D_{without MF} - D_{with MF}$) was found in the range of 17 and 34% Fe₃O₄. It means that the drug inner the ferrogel was obstructed more strongly in this range, rather than the others, ex. 8–17% and 34–68%. This indicates that the diffusion coefficient (D) plays a rather important role to evaluate the behavior of drug inner the ferrogel.

In addition, as shown in a magnetic-sensitive behavior map of Fig. 1(c), it showed an increase with Fe₃O₄ until 17%, indicating the region of increasing sensitivity (Region A). Subsequently, a plateau profile is reached while Fe₃O₄ is lying between 17 and 34%, indicating the magnetic-sensitive behavior reaching a saturation region (Region B). However, the magnetic-sensitive behaviors decreased with further addition of Fe₃O₄ up to 68% (Region C), indicating a decreased sensitivity to a given magnetic stimulation. These results indicated that the best magnetic-sensitive behaviors occur for the 10% PVA-ferrogels with 17–34% Fe₃O₄ concentration.

3.1.1. Effects of space restriction

The reason for such a dependence of Fe₃O₄ concentration on the evolution of the magnetic-sensitive map may be accountable for as a result of space restriction and magnetization. In Fig. 2(a), a model with a fixed volume of the unit cell is adapted for schematically illustrating the spatial arrangement

of the magnetic particles (presumed to be uniformly distributed) in the ferrogels (namely PVA10-MP17, PVA10-MP34 and PVA10-MP68). Here, the SEM cross-sectional image of the PVA10-MP17, PVA10-MP34, and PVA10-MP68 ferrogels, Fig. 2(b), in corresponding to model in Fig. 2(a) shows that the magnetic particles are well-dispersed in the PVA hydrogel, and it seems to be intertwined with Fe₃O₄ particles. The volume fraction, $V_f(\text{Fe}_3\text{O}_4)$ of Fe₃O₄ particles in the ferrogel and the number of Fe₃O₄ particles for unit volume of the ferrogel (No. Fe₃O₄) in the unit cell can be calculated as follows:

$$V_f(\text{Fe}_3\text{O}_4) = \frac{W_{\text{Fe}_3\text{O}_4}/\rho_{\text{Fe}_3\text{O}_4}}{V_{\text{ferrogel}}} \times 100\%(\text{v/v}\%) \quad (6)$$

$$\text{No.}(\text{Fe}_3\text{O}_4) = \frac{V_f(\text{Fe}_3\text{O}_4)}{4/3\pi r^3} \quad (7)$$

where $\rho_{\text{Fe}_3\text{O}_4}$ is the density of Fe₃O₄ particles (5.2 g/cm³); $W_{\text{Fe}_3\text{O}_4}$ means the total addition weight of the Fe₃O₄ particles in the ferrogel. Therefore, $W_{\text{Fe}_3\text{O}_4}/\rho_{\text{Fe}_3\text{O}_4} = V_{\text{Fe}_3\text{O}_4}$ represents the total volume of Fe₃O₄ in the ferrogel. $4/3\pi r^3$ indicates the volume of a Fe₃O₄ particle if the particle is assumed to be spherical. The total number of the Fe₃O₄ particles is $V_{\text{Fe}_3\text{O}_4}/4/3\pi r^3$ where r is the radius of the iron oxide particle and is assumed to have an average diameter of 250 nm, i.e., $r = 125$ nm. For the PVA10-MP17 ferrogel, there are 17.1 Fe₃O₄ particles in the unit cell (1 μm^3), 33.3 Fe₃O₄ particles in the PVA10-MP34 ferrogel, and 58.7 Fe₃O₄ particles in the PVA10-MP68 ferrogel, which are schematically shown in the Fig. 2(a). In order to conveniently and clearly express the relative number of the Fe₃O₄ particles in a basic unit cell, a model unit cell with a volume of 600 nm³ was used, as displayed in Fig. 2(a), and there are ca. 3.69 Fe₃O₄ particles in the given volume of the model cell for PVA10-MP17 ferrogel, 7.19 and 12.69 Fe₃O₄ particles for PVA10-MP34 and PVA10-MP68 ferrogels, respectively. Furthermore, V_{ferrogel} represents the bulk volume of the ferrogel determined by the length, width, and thickness of various ferrogels.

In addition, the average porosity (%) of these ferrogels can be measured by a pycnometer and calculated by Eqs. (3)–(5), where the porosity in the ferrogel decreased with increasing Fe₃O₄, as illustrated in Fig. 3(a). This indicates that increase in the concentration of Fe₃O₄ caused a reduction of porosity, and the lower porosity will slower the permeation rate of the model drug in the absence of MF, i.e., MF “OFF”. Moreover, it was found that the porosity of the ferrogel decreases linearly with the volume fraction occupied by iron oxide. The variation of those two parameters can be fitted by following equation:

$$\text{Porosity}(\%) + V_f(\text{Fe}_3\text{O}_4) (\text{v/v}\%) + x = 100\%$$

where $x = 33.6$ (+/–1.8) % may be interpreted as the volume fraction of organic matrix (i.e. PVA, and DMSO).

Although greater amount of Fe₃O₄ particles can increase the magnetization of the ferrogel, the space available for the Fe₃O₄ particles to freely move (where the available free volume per nanoparticle (V_{free}) was defined as below) will correspondingly decrease. While the available free volume per nanoparticle for

the Fe_3O_4 particles is too small, it will inhibit the movement of the Fe_3O_4 particles in the unit cell, thus, the magnetic-sensitive behavior will decrease even though those particles exhibited high magnetization (M_s).

The available free volume of each magnetic nanoparticle can be calculated by Eq. (8):

$$\text{Available free volume per nanoparticle } (V_{\text{free}}) = \frac{\text{Porosity}(\%) \times V_{\text{ferrogel}}}{\text{No.}(\text{Fe}_3\text{O}_4)} \quad (8)$$

As given in Fig. 3(b), V_{free} is decreased in a power-law-dependent manner with increasing Fe_3O_4 concentration. V_{free} in the PVA10-MP3.75 ferrogel ($33.88 \mu\text{m}^3$) is about 30 times

higher than that in the PVA10-MP68 ferrogel ($0.95 \mu\text{m}^3$), calculated by Eq. (8).

3.1.2. Effects of magnetization

In regard to the magnetization of the Fe_3O_4 in the ferrogels, the interaction energy (E_{int}) between two particles with identical moment magnetization (M_s) can be given as follows [22–23]:

$$E_{\text{int}} \propto \frac{M_s^2 (3\cos\psi_1\cos\psi_2 - \cos\alpha)}{\delta^3} \quad (9)$$

where δ (μm) is the center-to-center distance between two neighboring particles, which is calculated by $d+2r$; r is the

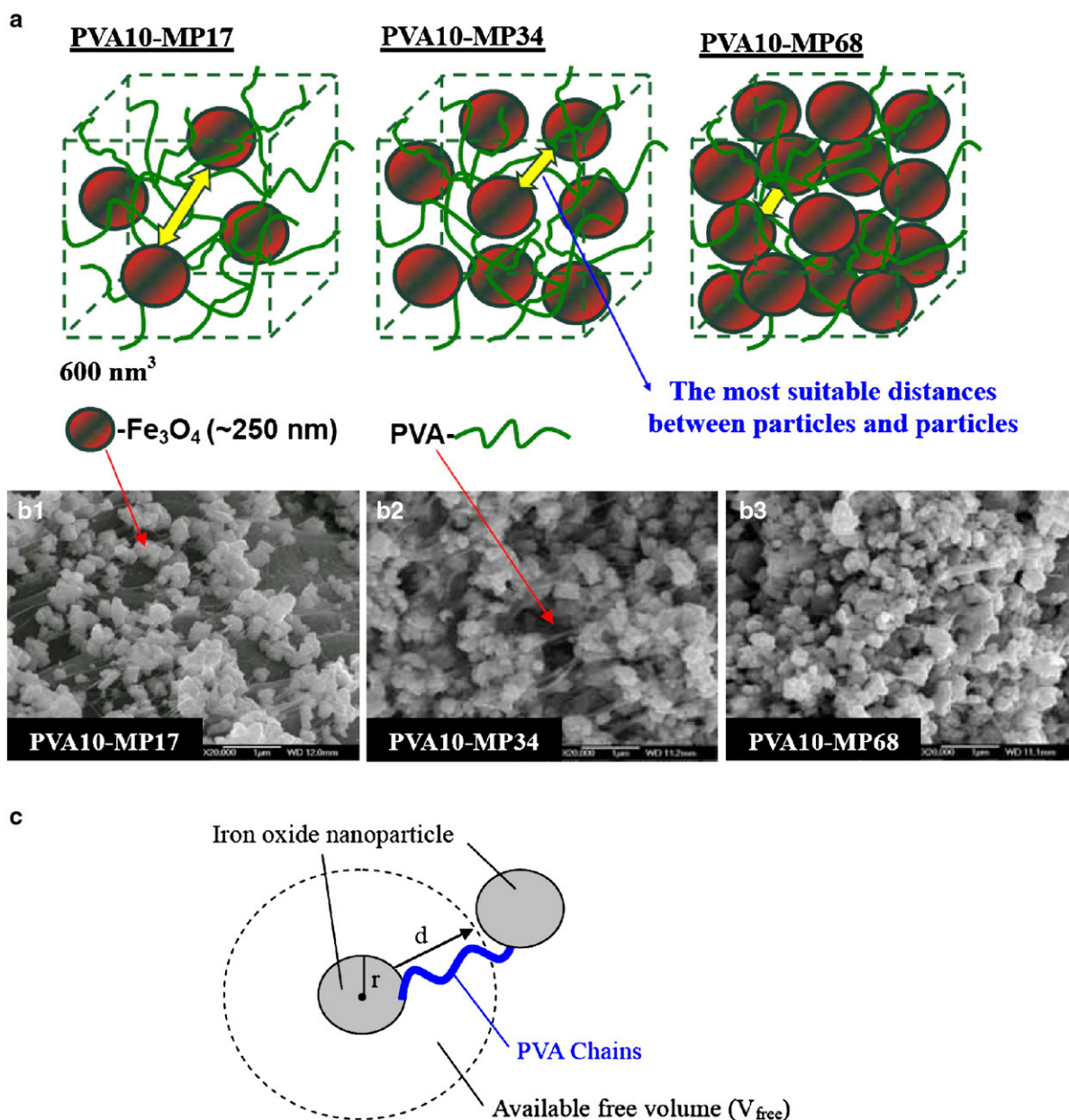


Fig. 2. (a) Models of the unit cell (600 nm^3) of PVA-based ferrogels which Fe_3O_4 particles distributed; (b) SEM cross-section image of PVA10-MP34 ferrogel. (c) Schematic drawing of the relationship of surface-to-surface distance between two neighboring particles (d) and available free volume per nanoparticle (V_{free}).

average radius of Fe_3O_4 particles (ca. 125 nm); d is the surface-to-surface distance between two neighboring particles; ψ_1 and ψ_2 are the angles between δ and two moments, respectively; α is the angle between the two moments. However, d is hardly precisely measured. Therefore, a rough measurement was performed by SEM as observed in Fig. 2(b). For example, the average d value in the PVA10-MP34 ferrogel was about 1 μm that is approximately the same order of magnitude to that (0.75 μm) calculated from the following presumed model (see Fig. 2(c) and Eq. (10)). From the schematic drawing, it can be found that V_{free} is equal to $\frac{4\pi}{3} [(d+r)^3 - r^3]$.

Therefore,

$$d = \left(\frac{3}{4\pi} V_{\text{free}} + r^3 \right)^{1/3} - r \quad (10)$$

Therefore, the average distance (d) between particles will be used in this work to evaluate the E_{int} . The M_s of various ferrogels was measured by a vibrating sample magnetometer (VSM, Toei VSM-5, USA). The M_s increased with the Fe_3O_4 addition, as illustrated by the magnetization curves in Fig. 4. Further, $(3\cos\psi_1\cos\psi_2 - \cos\alpha)$ and other interrelated factors

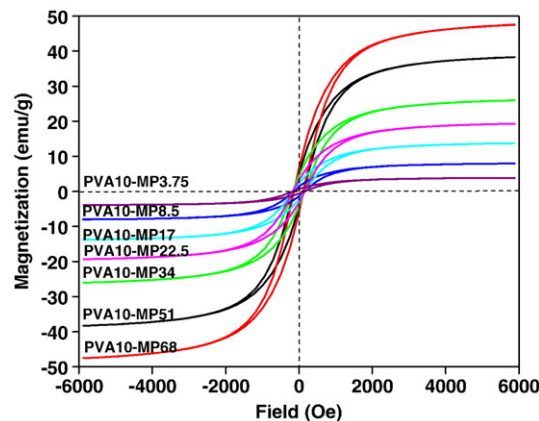


Fig. 4. Hysteresis loop analysis of the ferrogels incorporated with various Fe_3O_4 additions measured by VSM.

were hypothesized as constant (ϕ). Hence, to combine Eq. (9) with Eq. (10), the interaction energy (E_{int}) can be well characterized using Eq. (11)

$$E_{\text{int}} = \frac{M_s^2}{(d+2r)^3} \phi \quad (11)$$

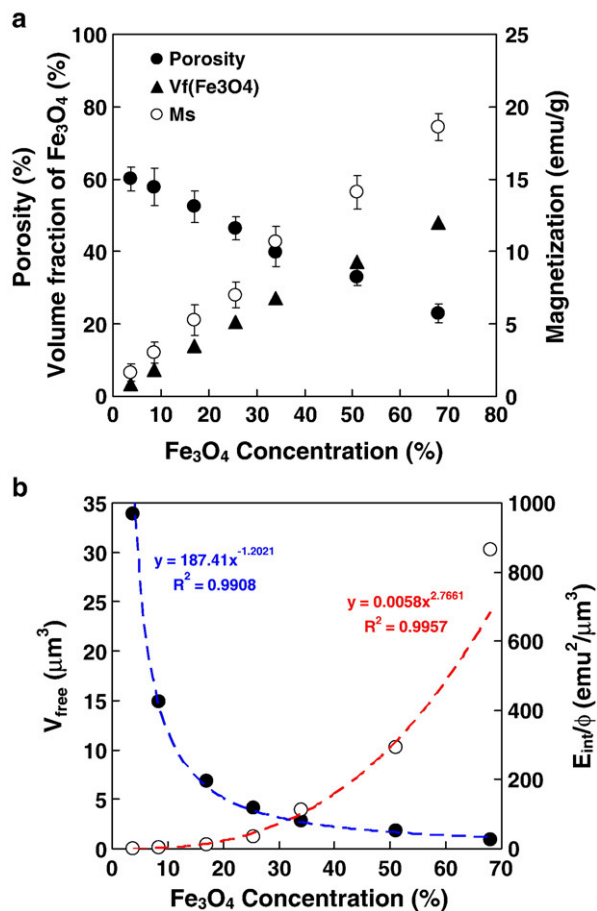


Fig. 3. Comparison of (a) porosity (%), volume fraction of Fe_3O_4 particles ($V_f(\text{Fe}_3\text{O}_4)$) and magnetization (M_s); (b) both available free volume per nanoparticle (V_{free}) and interaction energy (E_{int}) of ferrogels dependence of various Fe_3O_4 concentrations.

The $E_{\text{int}}-\text{Fe}_3\text{O}_4$ concentration correlation, shown in Fig. 3(b), shows that the interaction energy is increased, followed by a power-law dependence, with increasing Fe_3O_4 concentration. The interaction energy in the PVA10-MP68 ferrogel ($865.68 \text{ emu}^2/\mu\text{m}^3 \times \phi$) is about 3150 times higher than that in the PVA10-MP3.75 ferrogel ($0.27 \text{ emu}^2/\mu\text{m}^3 \times \phi$), as shown in Fig. 3(b).

Based on these calculations, it is clearly demonstrated that the lower Fe_3O_4 concentration leaves larger V_{free} but poorer interaction energy between the particles in the ferrogels, and vice versa, for the ferrogels with higher Fe_3O_4 concentration. Therefore, the “optimal” magnetic-sensitive behavior is virtually interplaying between the V_{free} and the interaction energy in the ferrogels. The concentration of the Fe_3O_4 for the optimal balance between the two factors can be obtained from the intersection of two power-law-dependent curves in Fig. 3 (b), where an amount of between 30 and 34% of the Fe_3O_4 was derived. This concentration range is exactly located within the saturation region of the magnetic sensitivity map (Region B) shown in Fig. 1(c). It can be anticipated that the ferrogels with Fe_3O_4 concentration in the range of 30–34% offer the best spatial configuration of the particles in the unit cell model facilitating both V_{free} and magnetization. By translating to what experimentally observed, the PVA10-MP34 ferrogel does display the optimal “opening-&-closure” configuration with respect to “on-off” MF operation and also illustrated the best magnetic-sensitive behavior, as evidenced in Fig. 1(a). In other words, the magnetic particles distributed in the PVA10-BM34 ferrogel presents the best spatial configuration for optimizing both V_{free} and magnetization among the other compositions.

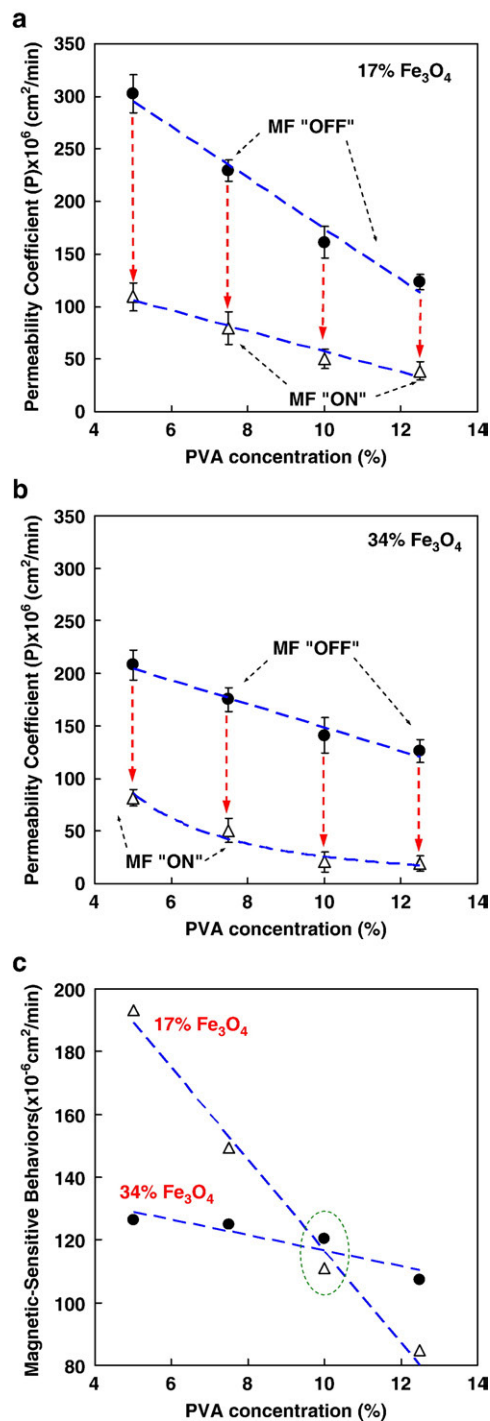


Fig. 5. Permeability coefficient of various PVA addition in "on" or "off" mode of a given magnetic field with (a) 17% Fe₃O₄ contents and (b) 34% Fe₃O₄ contents; (c) Comparison of magnetic-sensitive behaviors between 17% and 34% Fe₃O₄ contents.

3.2. Role of PVA content

Since the "closure" and "opening" configurations of the ferrogels are dependent solely on the operating mechanism of both magnetic particles and the polymeric phase, i.e., PVA, under the action (ON mode) and removal (OFF mode) of the magnetic field. The polymeric phase is virtually a passive phase

that intimately associated with the movement of magnetizing or de-magnetizing Fe₃O₄ nanoparticles in the ferrogel. However, PVA addition reduced the porosity and formed more rigid ferrogels and thus, the drug permeation rate, corresponding to P value, will surely reduce under on–off operation of the magnetic field. Thus, the change in the concentration of the polymeric phase in the ferrogels will affect its ability to effectively enclose and release an active ingredient from the ferrogels under a fixed amount of Fe₃O₄ concentration in a given strength of magnetic field. To elucidate the influence of the PVA on the magnetic-sensitive behavior in the ferrogels, PVA concentrations of 5%, 7.5%, 10%, and 12.5% were selected for the ferrogels with 17% and 34% Fe₃O₄ nanoparticles (hereinafter termed 17% and 34% Fe₃O₄ ferrogels), which has been shown in Fig. 1(b) to exhibit stable and excellent magnetic-sensitive behavior (Region B).

Fig. 5(a) and (b) shows the variation of P value of the ferrogels before (i.e., MF "OFF", P_{OFF}) and after (MF "ON", P_{ON}) an MF operation. For 17% Fe₃O₄ ferrogel, that the value of P_{OFF} decreased sharply with increasing PVA concentration [see Fig. 5(a)], but P_{ON} decreased slowly with PVA concentration. In addition, the change in the P value with respect to the PVA concentration for 34% Fe₃O₄ ferrogels exhibits similar trend before (MF "OFF"), and after (MF "ON") magnetization. However, compared with 17% Fe₃O₄ ferrogels, P_{ON} of 34% Fe₃O₄ ferrogels decreased slightly (followed by a power-law dependence) with the increased PVA concentration, in Fig. 5(b). It displays a "saturation" region while increasing PVA over the range of 10–12.5%, implying that the best "closure" configuration in this system is lying between 10 and 12.5% PVA content. According to these findings, it can be found that the magnetic sensitivity is decreased considerably and linearly with increasing PVA concentration for the 17% Fe₃O₄ ferrogels but decreased relatively slowly for the 34% Fe₃O₄ ferrogels as shown in Fig. 5(c), indicating that the magnetic-sensitive behavior of the ferrogels is proportionally decreased by the addition of PVA. However, the effect of PVA appears to be less pronounced in the 34% Fe₃O₄ ferrogel, since its magnetic

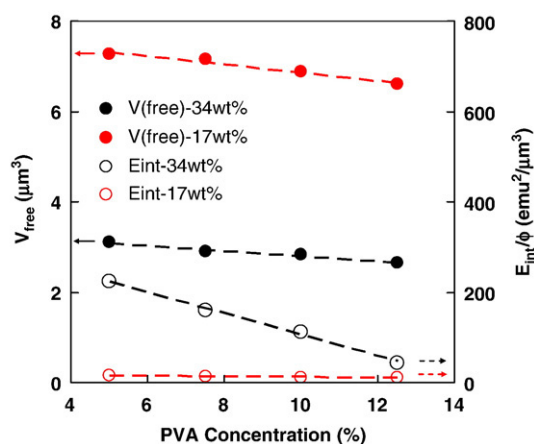


Fig. 6. Correlation of both available free volume per nanoparticle (V_{free}) and interaction energy (E_{int}) in the ferrogels between 17% Fe₃O₄ and 34% Fe₃O₄ contents.

behavior does not display remarkable fluctuation or change with increasing PVA as compared to that with 17% Fe₃O₄ ferrogel.

The above-mentioned results can be further explained in terms of the effect of space restriction and magnetization, as illustrated in Fig. 6 for 17% and 34% Fe₃O₄ ferrogels, respectively. PVA addition in both ferrogels (i.e., 17% and 34% Fe₃O₄) leads to a reduction in both V_{free} (calculated using Eq. (8)) and the interaction energy (E_{int}). Consequently, P value under MF “OFF” is decreased sharply. In the meantime, it also reveals a reduction in the permeation rate of the drug from the ferrogels with increasing PVA under MF “ON” operation due to lower porosity, and these have been experimentally supported in Fig. 5(a) and (b). It is evidenced that increasing PVA not only reduces V_{free} but also weakens E_{int} of the magnetic particles in the ferrogels. Therefore, both V_{free} and E_{int} are decreased linearly with PVA concentration.

In addition, 17 wt.% series ferrogel exhibited better magnetic sensitivity in the lower concentration region of PVA (ex. 5 wt.% PVA) compared to 34 wt.% series ferrogel, because the V_{free} of 17 wt.% ($7.3 \mu\text{m}^3$) is larger than that of 34 wt.% ($3.1 \mu\text{m}^3$), as shown in Fig. 6. It means that iron oxide is easier to move in the 17 wt.% series ferrogel than that in the 34 wt.% series. However, the interaction energy (E_{int}) of 17 wt.% series ferrogel ($15.6 \text{ emu}^2/\mu\text{m}^3\phi$) is much smaller than that of 34% series ($224.8 \text{ emu}^2/\mu\text{m}^3\phi$). Therefore, E_{int} value in the 17 wt.% series might be not large enough for magnetic sensitivity with higher PVA addition, which is the reason that the magnetic sensitivity decreased so sharply in the 17 wt.% series. In contrast, 34 wt.% series ferrogel displays smaller V_{free} but higher E_{int} , which means that they exhibit a higher E_{int} but limited V_{free} . That is why the magnetic sensitivity of 34 wt.% series is higher than 17 wt.% series (higher E_{int} and lower V_{free}), although both factors of 17 wt.% and 34 wt.% series were decreased with increasing PVA.

Moreover, as compared to Fig. 3(b) with an increase of Fe₃O₄, E_{int} increased but V_{free} decreased, it is clear to realize that both the Fe₃O₄ and PVA constituents play different roles for drug permeation behavior and magnetic-sensitive behavior of the resulting ferrogels. Accordingly, the resulting ferrogels can be manipulated externally and magnetically with a precise control of the opening and closure of pore configuration within the network structure of the ferrogels.

4. Concluding remarks

The effect of the Fe₃O₄ and matrix PVA on the magnetic-sensitive behavior of ferrogels was systematically investigated. Magnetic-sensitive behavior map in terms of Fe₃O₄ concentration was constructed and the behavior reached a “saturation” region in the range of 17–34% Fe₃O₄. Below or above that region, a reduction in the magnetic-sensitive behavior was observed. Both the concentration dependence of the magnetic-sensitive behavior with respect to PVA and Fe₃O₄ can be explainable in terms of a space restriction model (translated into available free volume) and magnetization (translated into the interaction energy). These two factors impose opposite effect to the resulting magnetic-sensitive behavior, and accordingly, an

optimal combination of both available free volume and interaction energy can be found for the ferrogels with a composition of 17–34% Fe₃O₄ and 10–12.5% PVA. It is anticipated that the ferrogels with an optimal mixture of PVA and Fe₃O₄ display a magnetic-sensitive behavior that permits the ferrogels technologically applicable as a microdevice for delivery of therapeutic drugs in a highly controllable manner.

Acknowledgement

The authors gratefully acknowledge the National Science Council of the Republic of China for its financial support through Contract No. NSC-95-2221-E-009-126.

References

- [1] P.M. Xulu, G. Filipcsei, M. Zrínyi, Preparation and responsive properties of magnetically soft poly(*N*-isopropylacrylamide) gels, *Macromolecules* 33 (2000) 1716–1719.
- [2] J.Y. Kim, S.B. Lee, S.J. Kim, Y.M. Lee, Rapid temperature/pH response of porous alginate-g-poly(*N*-isopropylacrylamide) hydrogels, *Polymer* 43 (2002) 7549–7558.
- [3] Y. Deng, W. Yang, C. Wang, S. Fu, A novel approach for preparation of thermoresponsive polymer magnetic microspheres with core-shell structure, *Adv. Mater.* 15 (2003) 1729–1732.
- [4] I. Csetneki, G. Filipcsei, M. Zrínyi, Smart nanocomposite polymer membranes with on/off switching control, *Macromolecules* 39 (2006) 1939–1942.
- [5] R. Fernandes, L.Q. Wu, T. Chen, H. Yi, G.W. Rubloff, R. Ghodssi, W.E. Bentley, G.F. Payne, Electrochemically induced deposition of a polysaccharide hydrogel onto a patterned surface, *Langmuir* 19 (2003) 4058–4062.
- [6] S.Y. Kim, Y.M. Lee, Drug release behavior of electrical responsive poly(vinyl alcohol)/poly(acrylic acid) IPN hydrogels under an electric stimulus, *J. Appl. Polym. Sci.* 74 (1999) 1752–1761.
- [7] K. Haraguchi, T. Takehisa, S. Fan, Effects of clay content on the properties of nanocomposite hydrogels composed of poly(*N*-isopropylacrylamide) and clay, *Macromolecules* 35 (2002) 10162–10171.
- [8] R. Mohr, K. Kratz, T. Weigel, M. Lucka-Gabor, M. Moneke, A. Lendlein, Initiation of shape-memory effect by inductive heating of magnetic nanoparticles in thermoplastic polymers, *PNAS* 103 (2006) 3540–3545.
- [9] E.C. Muniz, G. Geuskens, Compressive elastic modulus of polyacrylamide hydrogels and semi-IPNs with poly(*N*-isopropylacrylamide), *Macromolecules* 34 (2001) 4480–4484.
- [10] T.G. Park, H.K. Choi, Thermally induced core-shell type hydrogel beads having interpenetrating polymer network (IPN) structure, *Macromol. Rapid Commun.* 19 (1998) 167–172.
- [11] D. Szabó, I. Czákó-Nagy, M. Zrínyi, A. Vértvs, Magnetic and Mössbauer studies of magnetite-loaded polyvinyl alcohol hydrogels, *J. Colloid Interface Sci.* 221 (2000) 166–172.
- [12] Z. Lu, M.D. Prouty, Z. Guo, V.O. Golub, C.S.S.R. Kumar, Y.M. Lvov, Magnetic switch of permeability for polyelectrolyte microcapsules embedded with Co@Au nanoparticles, *Langmuir* 21 (2005) 2042–2050.
- [13] O. Saslawski, C. Weingarten, J.P. Benoit, P. Couvreur, Magnetically responsive microspheres for the pulsed delivery of insulin, *Life Sci.* 42 (1988) 1521–1528.
- [14] T.Y. Liu, S.H. Hu, T.Y. Liu, D.M. Liu, S.Y. Chen, Magnetic-sensitive behavior of intelligent ferrogels for controlled release of drug, *Langmuir* 22 (2006) 5974–5978.
- [15] T.Y. Liu, S.H. Hu, K.H. Liu, D.M. Liu, S.Y. Chen, Preparation and characterization of smart magnetic hydrogels and its use for drug release, *J. Magn. Magn. Mater.* 304 (2006) e397–e399.
- [16] M. Zrínyi, Intelligent polymer gels controlled by magnetic fields, *Colloid Polym. Sci.* 278 (2000) 98–103.
- [17] T. Hatakeyama, J. Uno, C. Yamada, A. Kishi, H. Hatakeyama, Gel-sol transition of poly(vinyl alcohol) hydrogels formed by freezing and thawing, *Thermochimica Acta* 431 (2005) 144–148.

- [18] D.K. Singha, A.R. Raya, Controlled release of glucose through modified chitosan membranes, *J. Membrane Sci.* 155 (1999) 107–112.
- [19] M.C. Yang, T.Y. Liu, The permeation performance of polyacrylonitrile/polyvinylidene fluoride blend membranes, *J. Membrane Sci.* 226 (2003) 119–130.
- [20] M. Miyajima, A. Koshika, J. Okada, M. Ikeda, Mechanism of drug release from poly(L-lactic acid) matrix containing acidic or neutral drugs, *J. Control. Release* 60 (1999) 199–209.
- [21] T.Y. Liu, S.Y. Chen, J.H. Li, D.M. Liu, Study on drug release behaviour of CDHA/chitosan nanocomposites—effect of CDHA nanoparticles, *J. Control. Release* 112 (2006) 88–95.
- [22] J. Chatterjee, Y. Haik, C.J. Chen, Polyethylene magnetic nanoparticle: a new magnetic material for biomedical applications, *J. Magn. Mater.* 246 (2002) 382–391.
- [23] J. Dai, J.Q. Wang, C. Sangregorio, J. Fang, E. Carpenter, J. Tang, Magnetic coupling induced increase in the blocking temperature of γ -Fe₂O₃ nanoparticles, *J. Appl. Phys.* 87 (2000) 7397–7399.